Received: 12 October 2021 | Revised: 11 January 2022 | Accepted: 20 January 2022

DOI: 10.1111/cas.15275

Cancer Science WILEY

ORIGINAL ARTICLE

Long noncoding RNA *EIF1AX-AS1* promotes endometrial cancer cell apoptosis by affecting *EIF1AX* mRNA stabilization

Chengyu Lv[1,2] | Jiandong Sun[1] | Yuhong Ye[3,4] | Zihang Lin[1] | Hua Li[1,3] | Yue Liu[1,3] | Kaien Mo[1] | Weiwei Xu[1] | Weitao Hu[1] | Eman Draz[3,5] | Shie Wang[1,3]

[1]Key Laboratory of Stem Cell Engineering and Regenerative Medicine of Fujian Province University, Fujian Medical University, Fuzhou, China

[2]Department of Obstetrics and Gynecology, Fujian Maternity and Child Health Hospital, Affiliated Hospital of Fujian Medical University, Fuzhou, China

[3]Department of Anatomy, Histology and Embryology, School of Basic Medical Sciences, Fujian Medical University, Fuzhou, China

[4]Department of Pathology, The First Affiliated Hospital of Fujian Medical University, Fuzhou, China

[5]Human Anatomy and Embryology Department, Suez Canal University, Egypt

Correspondence
Shie Wang, Department of Human Anatomy, Histology and Embryology, School of Basic Medical Sciences, Fujian Medical University, No.1 Xuefu North Road, University Town, Minhou County, Fuzhou 350122, China.
Email: shiewang@fjmu.edu.cn

Funding information
Startup Fund for scientific research of Fujian Medical University, Grant/Award Number: 2018QH2016; Science and Technology Innovation Foundation of Fujian Province, Grant/Award Number: 2017Y9114

Abstract

Long noncoding RNAs (lncRNAs) have been found to play an important role in the occurrence and development of endometrial carcinoma (EC). Here, using RNA sequencing analysis, we systemically screened and identified the lncRNA eukaryotic translation initiation factor 1A, X-linked (EIF1AX)-AS1, which is aberrantly downregulated in clinical EC tissues and closely correlated with tumor type. *EIF1AX-AS1* markedly inhibited EC cell proliferation and promoted apoptosis *in vitro* and *in vivo*. Mechanistically, *EIF1AX-AS1* interacts with *EIF1AX* mRNA and poly C binding protein 1 (PCBP1), which promote *EIF1AX* mRNA degradation. Intriguingly, by interacting with internal ribosome entry site-related protein Y-box binding protein 1 (YBX-1), EIF1AX promotes c-Myc translation through the internal ribosome entry site pathway. c-Myc promotes *EIF1AX* transcription and thus forms a feed-forward loop to regulate EC cell proliferation. Taken together, these data reveal new insights into the biology driving EC proliferation and highlights the potential of lncRNAs as biomarkers for prognosis and future therapeutic targets for cancer.

KEYWORDS
apoptosis, EIF1AX, endometrial cancer, long noncoding RNA, RNA binding protein

Abbreviations: CHX, cycloheximide; CPAT, coding potential assessment tool; EC, endometrial cancer; EIF1AX, eukaryotic translation initiation factor 1A, X-linked; GO, Gene Ontology; hnRNP, heterogeneous nuclear ribonucleoprotein; IGF2BP1, insulin-like growth factor 2 mRNA binding protein 1; IRES, internal ribosome entry site; KEGG, Kyoto Encyclopedia of Genes and Genomes; KH, K homology; lncRNA, long noncoding RNA; PCBP1, poly C binding protein 1; RACE, rapid amplification of cDNA ends; RBP, RNA-binding protein; RIP, RNA immunoprecipitation; RNA-seq, RNA sequencing; RT-qPCR, quantitative RT-PCR; YBX-1, Y-box binding protein 1.

Chengyu Lv, Jiandong Sun, and Yuhong Ye contributed equally to this work.

1 | INTRODUCTION

Endometrial cancer is the most common malignant tumor of the female reproductive system, with new EC cases accounting for 7% of all new malignant tumor cases in 2018.[1] Annual deaths from EC rank sixth among all malignant tumor deaths in female individuals, and deaths from EC are expected to account for 4% of all malignant tumor deaths in 2020.[1,2] Therefore, clarifying the detailed genetic mechanisms of EC is critical to aid in the development of effective strategies for both diagnosis and treatment.

Long noncoding RNAs are nonprotein-coding RNA molecules with various cellular functions. In the nucleus, lncRNAs can interact with chromatin and participate in transcriptional regulation processes. Long noncoding RNAs in the cytoplasm can regulate mRNA stability, translation, and intracellular signaling.[3] Xu et al found that the lncRNA *TLR8-AS1* activates NF-κB signaling and promotes ovarian cancer invasion and metastasis by maintaining *TLR8* mRNA stability in the cytoplasm.[4] In addition, lncRNAs often function by recruiting RBPs to aid in the regulation of the expression level of target genes or target proteins.[5,6] The lncRNA *EGFR-AS1* promotes proliferation and metastasis of renal cell carcinoma by recruiting the RBP HuR and maintaining the stability of *EGFR* mRNA.[7] What interests us is that many studies have confirmed that lncRNAs are closely related to tumor development and progression. Huang et al indicated that silencing of lncRNA *HOTAIR* significantly inhibits proliferation, migration, and invasion of EC cells and arrests the cell cycle in G_0/G_1 phase.[8] Therefore, the discovery of novel lncRNAs in EC could provide new targets for cancer therapy.

In this study, we undertook RNA-seq and identified the lncRNA *EIF1AX-AS1*, which is aberrantly downregulated in clinical EC tissues and closely correlated with tumor type of EC patients. Expression of lncRNA *EIF1AX-AS1* markedly inhibited cell proliferation and induced apoptosis *in vitro* and *in vivo*. Mechanistically, *EIF1AX-AS1* interacts with *EIF1AX* mRNA and PCBP1, which promote *EIF1AX* mRNA degradation. Intriguingly, through the interaction with the IRES-related protein YBX-1, EIF1AX promotes c-Myc translation through the IRES pathway. In addition, c-Myc promotes *EIF1AX* transcription and forms a feed-forward loop and EC cell proliferation.

2 | MATERIALS AND METHODS

2.1 | Tissue samples

Endometrial cancer tissues and adjacent noncancerous tissues were retrieved from the Department of Pathology at The First Affiliated Hospital of Fujian Medical University. The protocol for the research project has been approved by a suitably constituted Ethics Committee of the institution within which the work was undertaken and conforms to the provisions of the Declaration of Helsinki. The study approval reference is [2019]-096.

2.2 | RNA sequencing

For RNA-seq, tissues were collected and subjected to RNA extraction (EZNA Total RNA Kit I, Omega). Samples were sent to Allwegene Technology for sequencing.

2.3 | Immunohistochemistry

For immunohistochemical staining, formalin-fixed paraffin-embedded (Sigma, 252549; Sigma, 8002-74-2) EC tissues and adjacent noncancerous tissues were deparaffinized and rehydrated. The specimens were incubated in EDTA buffer (1 mM, pH 8.0) for antigen retrieval using a high-pressure method. Then, tissue sections were incubated overnight at 4°C with EIF1AX antibody (1:500), 3,3′-diaminobenzidine solution (ZSGB-BIO) was used to detect target proteins, which were conjugated with a peroxidase enzyme to form a brown precipitate.

2.4 | RNA FISH

RNA FISH was carried out with an *EIF1AX-AS1*-specific probe (GenePharma). Cells were fixed with 4% paraformaldehyde for 10 minutes and then incubated with *EIF1AX-AS1* probe overnight at 37°C. The cells were then washed and blocked by 3% BSA. The sequences of the *EIF1AX-AS1* probe are listed in Table S1.

2.5 | Cell culture, RNA interference, and stable cell lines

Human endometrial cancer EC cell lines HEC-1A and RL95-2 were provided by Cell Bank/Stem Cell Bank, Chinese Academy of Sciences. The cells were cultured in McCoy's 5A medium or DMEM/F12 medium (Gibco-BRL) containing 10% FBS (Gibco-BRL) at 37°C in humidified atmosphere containing 5% CO_2. The siRNAs were transfected in EC cells with Lipofectamine RNAiMAX (Invitrogen) following the manufacturer's instructions. To establish stable cell lines, lentivirus-mediated shRNA against *EIF1AX* (shEIF1AX), *EIF1AX-AS1* (shEIF1AX-AS1), and *YBX-1* (shYBX-1) and the lncRNA *EIF1AX-AS1* overexpression construct designed by Shengzhe Biotechnology were each transfected into EC cells according to the manufacturer's protocols. Infected cells were selected with puromycin treatment used in experiments.

2.6 | Mitochondrial membrane potential detection by JC-1

HEC-1A and RL95-2 cells were incubated with JC-1 (Beyotime) as previously reported[9] and examined under a Leica TCS SP5 confocal microscope. The relative fluorescence intensity of the red

and green light was calculated as an index reflecting mitochondrial activity.

2.7 | Cell proliferation assay

The CCK-8 (MedChemExpress) was used to assess cell proliferation ability in accordance with the manufacturer's instructions. Cells were seeded into 96-well culture plates at a density of 2×10^3 cells per well on the day before transfection. After 48 hours, the viability of EC cells was assessed using CCK-8 reagents from five replicates in three independent experiments.

2.8 | RNA pulldown assay

Biotin-labeled lncRNA-*EIF1AX-AS1* and its antisense RNA were *in vitro* transcribed with the Biotin RNA Labeling Mix (Invitrogen) and SP6/T7 RNA polymerase (Invitrogen). After treatment with RNase-free DNase I (Roche), biotinylated RNAs were purified with the RNeasy Mini Kit (Qiagen) and incubated with the indicated cell lysates for 1 hour at 4°C. Streptavidin-agarose beads (Invitrogen) were added to each tube and samples were held for 1 hour at room temperature. The retrieved proteins were evaluated by western blot analysis.

2.9 | RNA immunoprecipitation

We undertook RIP experiments using the Pierce Magnetic RNA-Protein Pull-Down Kit (Thermo Fisher Scientific) in accordance with the manufacturer's instructions. HEC-1A and RL95-2 cells were lysed and cell lysates were incubated with PCBP1 Ab (2 μg Ab/sample). An aliquot of lysate was removed as an input control. RNA enrichment was determined by RT-qPCR and normalized to the input control.

2.10 | 5′ and 3′ RACE

We used 5′ and 3′ RACE to determine the transcriptional initiation and termination sites of lncRNA *EIF1AX-AS1* using the SMARTer RACE cDNA Amplification Kit (Clontech) in accordance with the manufacturer's instructions. The primers used for the PCR of the RACE analysis are listed in Table S2.

2.11 | mRNA decay measurements

The stability of the *EIF1AX* mRNA was assessed by adding 10 μg/mL actinomycin D into the cell culture medium to inhibit mRNA transcription. At the indicated time points, the relative amount of specific mRNA remaining in each sample could be correlated with mRNA degradation. Total RNA was extracted at indicated hours after actinomycin D (10 μg/mL) treatment.

2.12 | Cycloheximide chase measurements of RNH1 half-life

EIF1AX siRNA was transiently transfected into HEC-1A cells. Cycloheximide (100 ng/mL) was added to the DMEM culture medium, and incubation was continued for the indicated time. The cell lysates were submitted for western blot analysis using mouse anti-His mAb (Invitrogen), and western blot data were quantified using ImageJ software.

2.13 | Flow cytometry

Cells (1×10^6) were trypsinized and resuspended to obtain single-cell suspensions. Detached cells were fixed overnight at 4°C in 70% ethanol, then stained with propidium iodide (Cell Cycle Detection kit; KeyGen) and analyzed with a FACScan flow cytometer (BD Biosciences) and ModFit 3.0 software (Verity Software House). To detect apoptosis, cells were stained with fluorescein isothiocyanate-conjugated annexin V and propidium iodide (Apoptosis Detection kit; KeyGEN) as recommended by the manufacturer and analyzed by flow cytometry. Data were analyzed with FlowJo software (Tree Star).

2.14 | Quantitative RT-PCR analyses

HEC-1A and RL95-2 cells transfected with siRNA were collected and subjected to RNA extraction with an EZNA Total RNA Kit I. Synthesis of cDNA was carried out on a PCR amplifier (AB2720; Applied Biosystems) following the reverse transcription kit manual. Sequences of PCR primers are listed in Table S2.

2.15 | Western blot analysis

Cell lysates were prepared as previously reported.[9] Anti-EIF1AX, anti-YBX-1, and anti-PCBP1 were diluted to 1:1000. Information regarding Abs is listed in Table S1.

2.16 | Animal experiments

Four-week-old athymic nude mice were purchased from Shanghai SLAC Laboratory Animal Co., Ltd. Experimental protocols concerning mice handling were under the approval of the Institutional Animal Care and Use Committee of Fujian Medical University. Mice were randomly divided into two or three groups, with seven mice in each group. HEC-1A cells (5×10^5) with *EIF1AX-AS1* stable overexpression, *EIF1AX-AS1* and *EIF1AX* overexpression, or control cells were subcutaneously injected into the flank of mice. Mice were killed 4 weeks after the injection of cancer cells, and tumor weights were analyzed. Expression of EIF1AX in tumors was determined by western blot analysis.

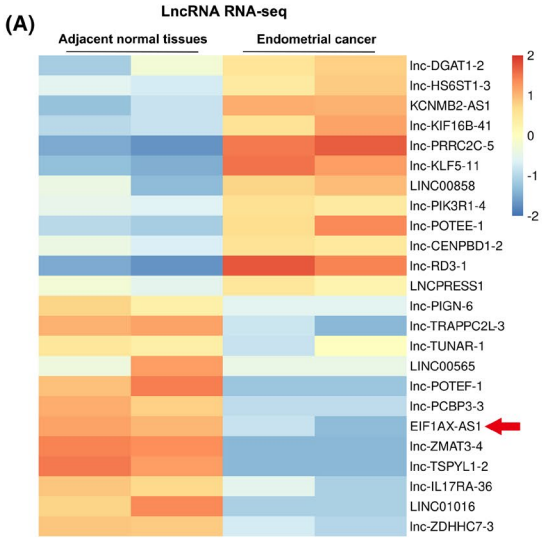

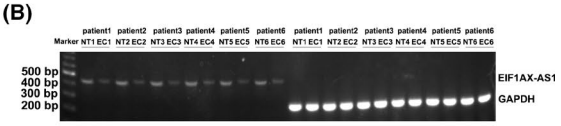

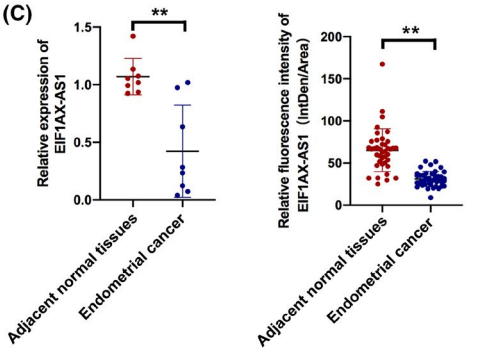

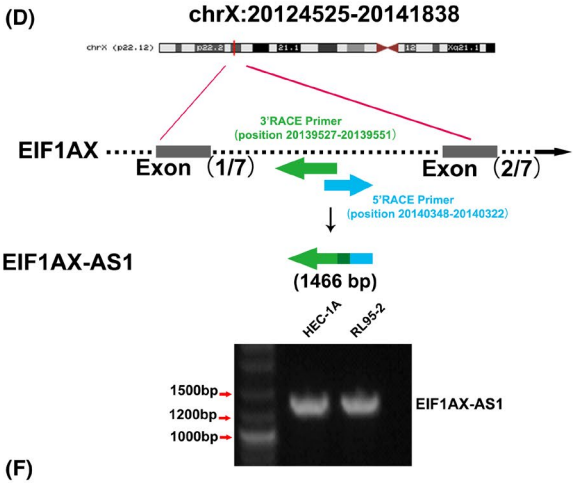

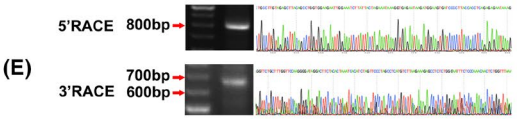

5'RACE identified transcript

AGATGCTTAATAAATATTTGTTGGTTTAAGTCACCTACCTCCTGTCGACTCCACCCTTAGTGAATAATAGGT
TCTGCTTTGGTTCCAAGGGGATAGGACTTCTACACTAAATCACATCTAGTTCCCTAGCCTCATGTCTTAAGA
AAGAGCCTCTCTGGGAATTTCTCCAAAACAACTCTGGTTTAAAGAATGTTGATGTCACTTTAATTGTTGTAC
ACTCAGACCTAGTCTCATTCATTCAACAGAGAATTTAAAGAACATCCCATTACATGGCAATAAAATACAAA
GGGGAGTGATCCGGGTATGGTTAATTCTGGTAAATTGACAAGTAATTAGTCTTTTCTTAAATAACATTTGA
GGCATACAAAAAATACAGCTAACATGATATACCTGGGAACCCATTACTCTGAATTTAAGAATTACAGCGCA
GATTGAGGTAAAGCCCTAATCACCTTTTACTCTCTTTTTGGAGGTAATCACCAGGCTGAGTTTGGTGTTTAT
CATTCCTGTACTGTCTGAAACCAATCAGTTCTTAGTTATCTTACTTAGAGGAATGGTACTTTTCATGACCTA
ATTTAAGTGTCCTCCATTTTTTTTTGCTGCTTCCAAGCTCTTCCCATGAGTCTCTTAGGGTCATTACCACTTA
CAGCCTTTTTCCTGCCTTTTGGAAATGGCTGCCAATGTGGTTTCCTTTCTGGAATGGGAGCAAAATGCTGT
GGAGAGGTAAGCTTATGTGGGGGCTAGGGGCAAAAAAAACATTGTGACTTTGGTCACCCCAGCTTACTG
ACTGTAATCAGTGAACTGATTTACTCACTGAAGCTAAGCGACTTACTTAACTTCTCTGAGCTTCAGGGAAC
TCATGGGTAAACTGGGA

3'RACE identified transcript

CTCTTTAAGGGTCTCTCCGAGAAAGAATTCTGTACTCCGATCCCCTTGATCTACACTAAATCACATCTTCAGG
ATAGGGGAACCTTGGTTTCGTCTTGGATAATAAGTGATTCCCACCTCAGCTGTCCTCCATCCACTGAATTTG
GTTGTTTATAAATAATTCGTAGATGATTAACAGTTCACGACGGTTAGGTTACTCTAATTCTGTCTATGATAA
GGACGGAACATCTCGAATGTCGGACCACCTTCTTAACCTTTAGAATAATGATCTTTATTTCCACTCTTATTC
TACCTTCACTAGGGGAATGGTGGAGTCTCTCTTATTTCCTAATATGTCTTCTTTTGACATTCTGAAATTTTAA
AAAACAAATATTGAGGTAGAAAAGGTTTTATTACTCGTCACTGACGTGGTTGAACACGTGTCTTGTGGAG
CTGGTTCATGGGATTCCCTATTTCATTATTCACTGTCGATGTTTCTCCTTTACACCATCTTAGGGACCTCGGT
CGACAGTTCATCTTTTCTCTCGTCTTCATCCGGACACAGTCCCCTCCCAAAGGAGATCTTACTTATTAGTTTC
CTCTGATGAATGCCTGATACTTCATACGAGGAGAGGACATCCTTTTATGTCATAAAAGGGATATAAATGAA
CGTGTTAAAAGAAGTTCAATATGCCGATAATTTTTACTGTCCTTGTGACATTTAGATATTTTCATTAAAGAA
ATCCTCACAAGACAAAAAACAAAAACAAAAAAAAAAAA

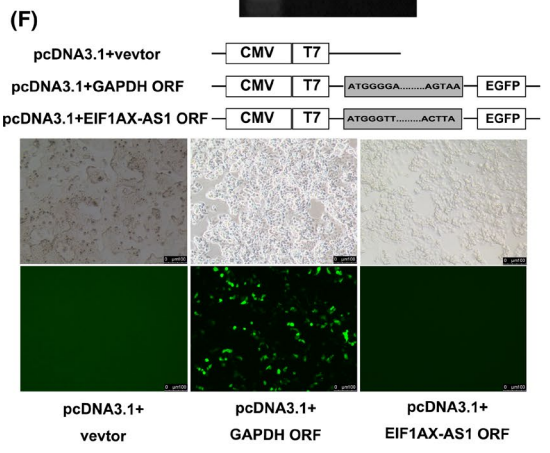

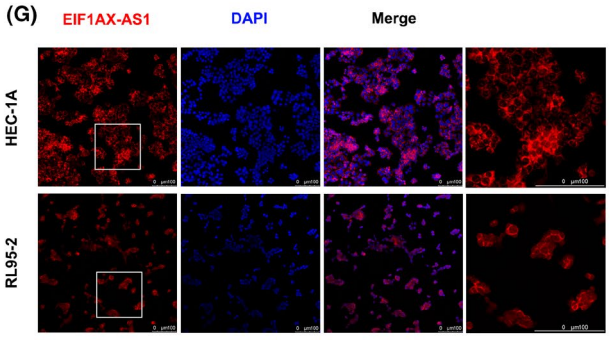

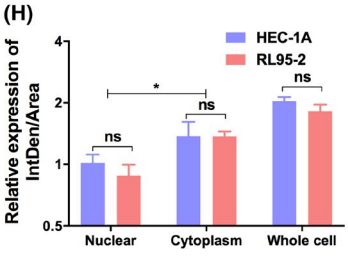

FIGURE 1 Identification of *EIF1AX-AS1*, which is downregulated in endometrial cancer (EC) tissues and correlated with a poor prognosis in EC. A, Heatmap showing different gene expressions between EC and adjacent normal tissues. B, *EIF1AX-AS1* expression between EC samples (EC) and adjacent normal tissues (NT) was compared using PCR analysis (n = 6). C, Left panel, quantitative RT-PCR analysis showed differentially expressed *EIF1AX-AS1* (red) in EC cells compared with adjacent normal tissues (blue; n = 8). Right panel, RNA FISH analysis indicated the differentially expression of *EIF1AX-AS1* (red) in EC cells compared with adjacent normal tissues (blue; n = 40). *t* test: $^{**}P < .01$. D, Schematic illustration showing that *EIF1AX-AS1* is derived from the intron region of the *EIF1AX* gene. E, Full-length sequence of *EIF1AX-AS1* was determined using 5′ and 3′ RACE assays. Kaplan-Meier analysis of the overall survival of EC patients with high or low *EIF1AX-AS1* expression. F, EIF1AX-AS1 ORF sequences were constructed and transfected into HEC-1A, positive control (pcDNA3.1 + GAPDH ORF), and negative control (pcDNA3.1 + vector). G, H, FISH analysis of *EIF1AX-AS1* in HEC-1A and RL95-2 cells using a biotin-labeled RNA probe. Nuclei were stained with DAPI. Scale bar = 100 μm. ImageJ software measured the quantification of RNA in the nucleus and cytoplasm. *t* test: ns, $P > .05$; $^{*}P < .01$. Bars indicate SD

TABLE 1 Relationship between expression of *EIF1AX-AS1* and clinicopathologic characteristics in patients with endometrial cancer

Characteristic	n	lncRNA *EIF1A-AS1*		*P* value
		Negative	Positive	
Specimen type				
Endometrial carcinoma	41	21	20	
Normal endometrium	30	0	30	.000
Tumor type				
Endometrioid carcinoma	21	7	14	
Serous carcinoma	20	14	6	.019
FIGO grade				
Low	16	2	14	
High	5	5	0	.001
FIGO stage				
I + II	29	13	16	
III + IV	12	8	4	.203
Invasive depth				
<1/2	21	9	12	
≥1/2	20	12	8	.272
Lymphovascular invasion				
Negative	24	11	13	
Positive	17	10	7	.412
Lymph node metastasis				
Negative	32	16	16	
Positive	9	5	4	.768
Ki-67 index				
Low expression	20	10	10	
High expression	21	11	10	.879

Abbreviations: Negative, FISH fluorescence intensity ≤30; Positive, FISH fluorescence intensity >30.

2.17 | Statistical analysis

Statistical analyses were undertaken using SPSS 20.0 statistical software (IBM) and GraphPad Prism 7.0 (GraphPad Software). Statistical tests used were the *t* test, one-way ANOVA, and χ^2 test. *P* values of less than .05 were considered to be significant.

3 | RESULTS

3.1 | Long noncoding RNA *EIF1AX-AS1* expression is decreased in human EC tissues and associated with tumor type

Long noncoding RNAs play key roles in tumor development. To identify lncRNAs that might play important roles in EC, we undertook RNA-seq analysis using EC and adjacent normal tissues. The results identified 1169 upregulated and 1841 downregulated lncRNAs, and the top 42 differentially expressed lncRNAs were depicted by a heatmap (Figure 1A). To validate the RNA-seq results, we randomly selected four downregulated lncRNAs with greater than 3-fold change ($P < .01$) and examined their expression in EC by RT-qPCR. Among the four lncRNAs, *EIF1AX-AS1* (transcript accession ENST00000424026) was the most decreased lncRNA in EC compared with adjacent normal tissues (Figure S1A). Downregulation of *EIF1AX-AS1* was further verified in the others EC and the HEC-1A and RL95-2 cell lines (Figures 1B and S1B). Thus, these two cell lines were chosen for subsequent experiments.

We next evaluated the expression level of lncRNA *EIF1AX-AS1* in 40 pairs of EC tissues and adjacent normal tissues. Most tumor tissues (32/40) showed lower levels of lncRNA *EIF1AX-AS1* compared with the adjacent normal tissues (Figures 1C and S1C). Moreover, increased lncRNA *EIF1A-AS1* was positively related to tumor type ($P = .001$), FIGO grade ($P = .001$), FIGO stage ($P = 0.203$), and invasive depth ($P = 0.272$; Table 1).

The RACE assay was used to identify the full sequence of *EIF1AX-AS1* in HEC-1A cells according to the primer sequence archived in the database of LNCipedia (https://lncipedia.org/). The results showed that *EIF1AX-AS1* is derived from the intron region between exons 1 and 2 of the *EIF1AX* gene (chrX: 20139547–20141012 reverse strand) (Figure 1D, E). In addition, the potential protein-coding capacity of lncRNA *EIF1AX-AS1* was predicted by the online prediction software ORF finder, which searches for ORFs (https://www.ncbi.nlm.nih.gov/orffinder/), and RNA CPAT (http://lilab.research.bcm.edu/cpat/index.php). The possible coding sequences of *EIF1A-AS1*, predicted by ORF finder and CPAT, were constructed on the EGFP fluorescent labeled vector, and the protein expression level was detected by immunofluorescence. Compared with the positive control (GAPDH ORF), the fluorescence signal of

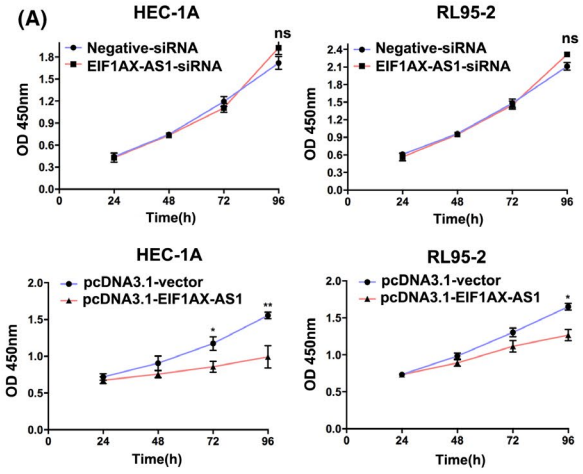
(A)
HEC-1A
RL95-2
Negative-siRNA
EIF1AX-AS1-siRNA
OD 450nm
Time(h)
ns
pcDNA3.1-vector
pcDNA3.1-EIF1AX-AS1

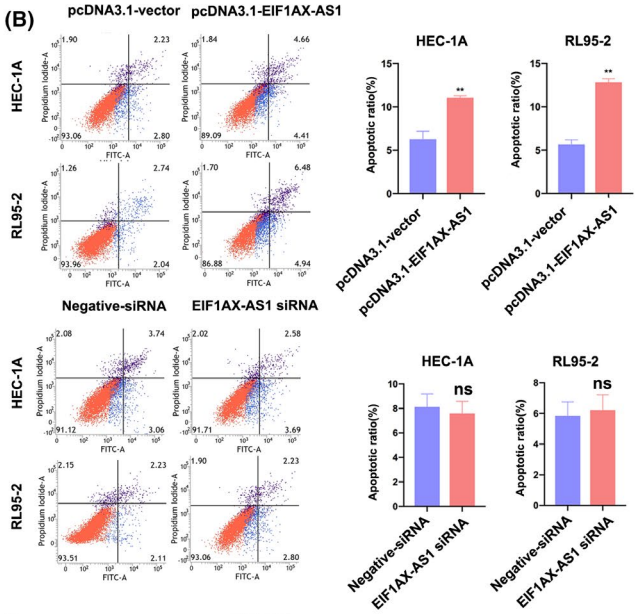
(B)
pcDNA3.1-vector
pcDNA3.1-EIF1AX-AS1
HEC-1A
RL95-2
Propidium Iodide-A
FITC-A
Apoptotic ratio(%)
Negative-siRNA
EIF1AX-AS1 siRNA
ns

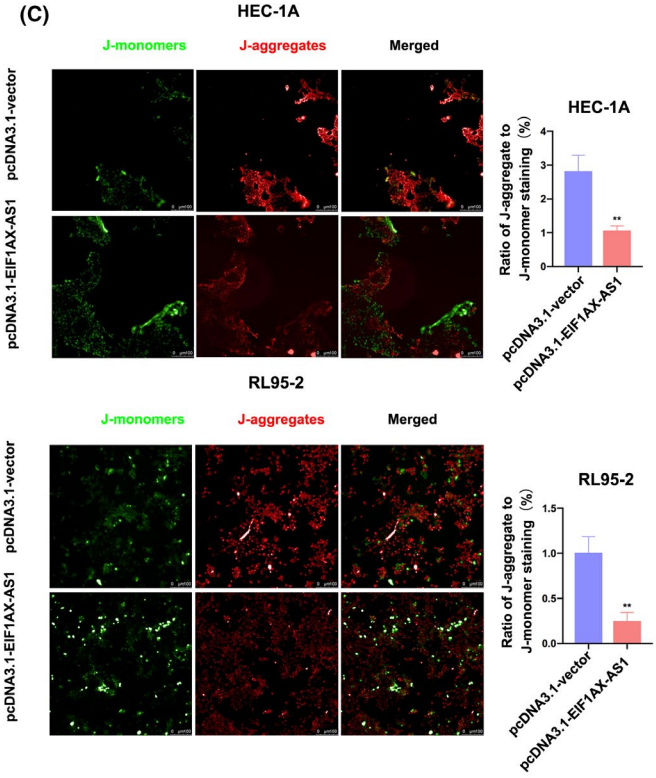
(C)
HEC-1A
RL95-2
J-monomers
J-aggregates
Merged
pcDNA3.1-vector
pcDNA3.1-EIF1AX-AS1
Ratio of J-aggregate to J-monomer staining (%)

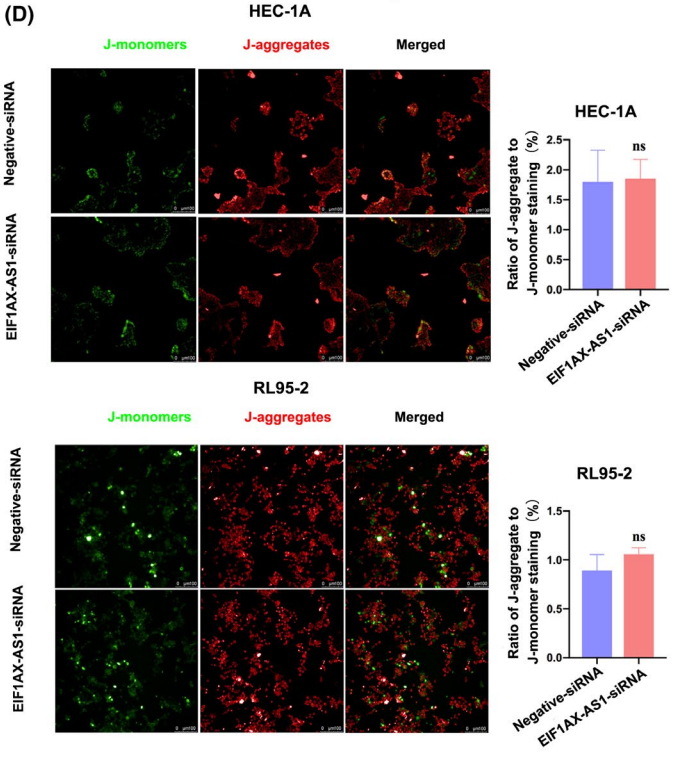
(D)
HEC-1A
RL95-2
J-monomers
J-aggregates
Merged
Negative-siRNA
EIF1AX-AS1-siRNA
Ratio of J-aggregate to J-monomer staining (%)
ns

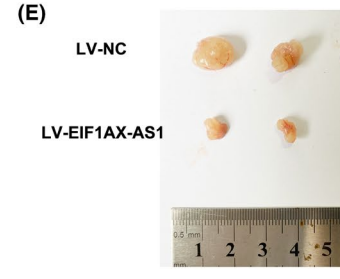
(E)
LV-NC
LV-EIF1AX-AS1

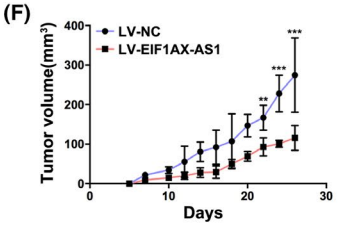
(F)
LV-NC
LV-EIF1AX-AS1
Tumor volume(mm³)
Days

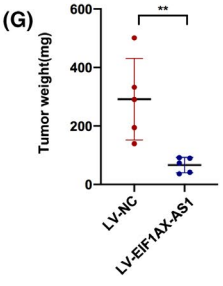
(G)
Tumor weight(mg)
LV-NC
LV-EIF1AX-AS1

FIGURE 2 *EIF1AX-AS1* knockdown suppressed proliferation activities and facilitates apoptosis of endometrial cancer (EC) cells *in vitro* and *in vivo*. A, CCK-8 detected the cell proliferation of EC cells at the indicated times. One-way ANOVA: $^{*}P < .05$; $^{**}P < .01$. B-D, After *EIF1AX-AS1* overexpression or knockdown, apoptosis of HEC-1A and RL95-2 cells was detected by annexin V-FITC and JC-1, respectively. *t* test: ns, $P > .05$, $^{**}P < .01$. E, Nude mice were given xenografts of *EIF1AX-AS1* overexpression (LV-EIF1AX-AS1) and control HEC-1A cells (LV-NC) (5×10^6 cells per site). Tumors were dissected and photographed after approximately 4 weeks (n = 5 per group). F, Growth curves of *EIF1AX-AS1* overexpression (LV-EIF1AX-AS1) tumors compared to control HEC-1A tumors (LV-NC). One-way ANOVA: $^{**}P < .01$; $^{***}P < .001$. G, Tumor weights were measured after tumor removal. *t* test: $^{**}P < .01$. Scale bar = 100 μm. Bars indicate SD

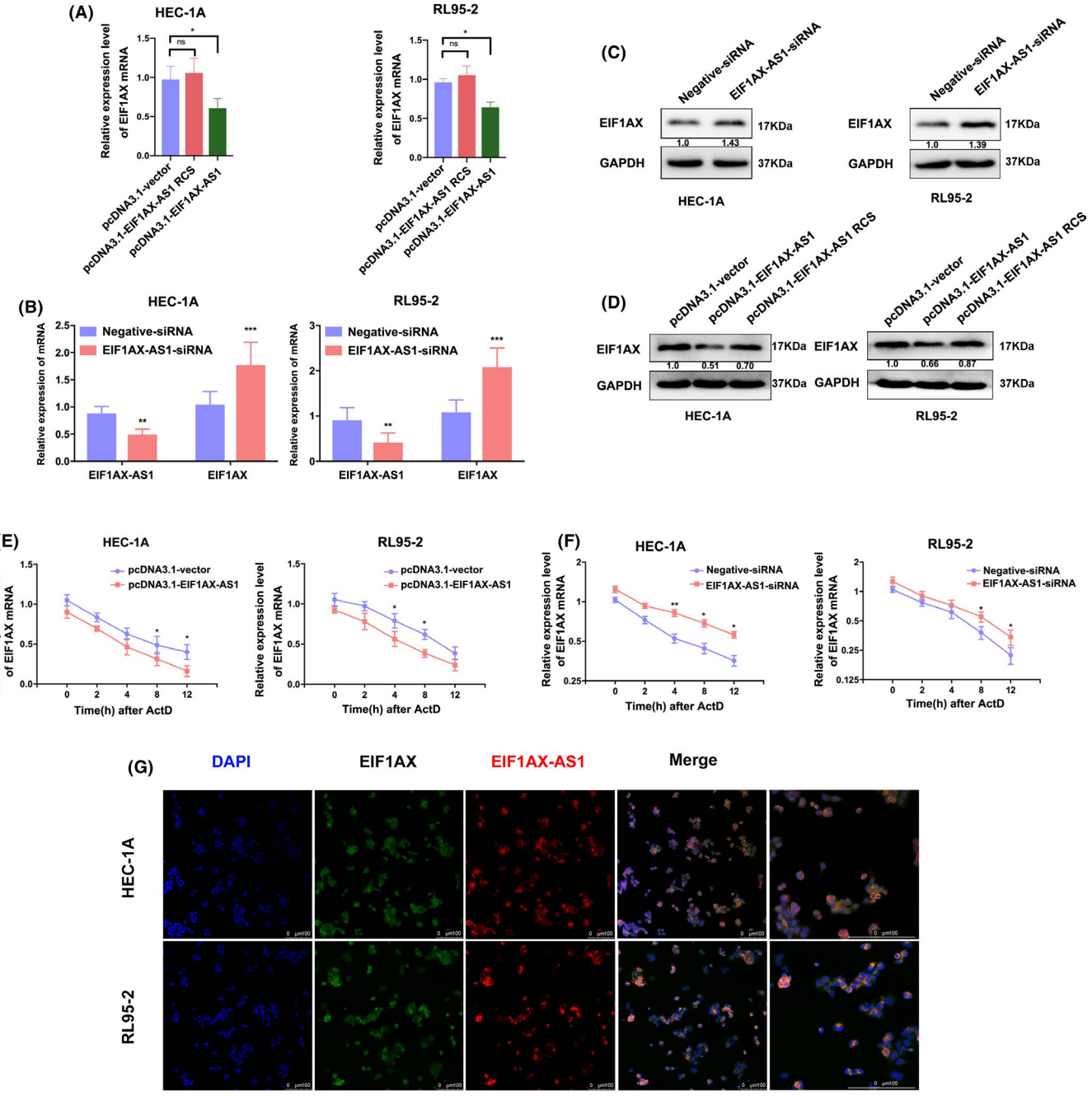

FIGURE 3 *EIF1AX-AS1* maintains *EIF1AX* mRNA instability. A, B, Expression of *EIF1AX* after *EIF1AX-AS1* overexpression vector transfection. Antisense RNA (pcDNA3.1-EIF1AX-AS1 RCS) was used as the negative control. One-way ANOVA: ns, $P > .05$; $^{*}P < .05$. C, D, *EIF1AX* expression after *EIF1AX-AS1* knockdown. *t* test: $^{**}P < 0.01$; $^{***}P < .001$. E, F, RNA stability assays were undertaken in EC cell lines using actinomycin D (ActD) to disrupt RNA synthesis, and the degradation rate of the *EIF1AX* mRNA was measured and calculated over 12 h. One-way ANOVA: $^{*}P < .05$; $^{**}P < .01$. G, RNA FISH analysis of *EIF1AX* mRNA (green) and *EIF1AX-AS1* (red) in RL95-2 and HEC-1A cells. Far right images show the colocalization of signals between the red signal (*EIF1AX-AS1*) and the green signal (*EIF1AX*). Scale bar = 100 μm. Bars indicate SD

the EIF1A-AS1 ORF group was not detected (Figure 1F), indicating that lncRNA *EIF1AX-AS1* was a noncoding RNA. Analysis using RNA FISH revealed that lncRNA *EIF1AX-AS1* was mainly located in the cytoplasm of HEC-1A and RL95-2 cells and in cells in clinical EC tissues (Figures 1G,H and S1D).

3.2 | Long noncoding RNA *EIF1AX-AS1* suppresses proliferation and increases apoptosis of EC cells

Based on the association between lncRNA *EIF1AX-AS1* and EC prognosis, we next explored the biological role of *EIF1AX-AS1* in EC cells *in vitro* and *in vivo*. Overexpression of *EIF1AX-AS1* significantly impaired the proliferative capacity of HEC-1A and RL95-2 cells ($P < .05$), as determined by CCK-8 cell proliferation assays (Figures 2A and S2A). However, flow cytometry and EdU assays indicated that the cell cycle and proliferation ability of EC cells was not changed after *EIF1AX-AS1* overexpression (Figure S2C,D). Annexin V-FITC and JC-1 staining showed that *EIF1AX-AS1* overexpression induced apoptotic cell death compared with the pcDNA3.1 vector group (Figure 2B-D). Collectively, these results indicate that overexpression of *EIF1AX-AS1* induced apoptotic cell death and impaired EC cell proliferation but had no influence on cell cycle progression. However, cell cycle progression, apoptosis, and proliferation of EC cells were not changed in cells with *EIF1AX-AS1* knockdown compared with the negative siRNA group (Figure S2B,E,F).

To investigate how *EIF1AX-AS1* impacts the proliferation of EC cells *in vivo*, we constructed HEC-1A stable cell lines with *EIF1AX-AS1* overexpression mediated by lentivirus (LV-EIF1AX-AS1) (Figure S2G). *EIF1AX-AS1* overexpression or control HEC-1A cells were subcutaneously injected into nude mice, and mice were monitored for several weeks. We found that tumor volumes and weights were smaller in the LV-EIF1AX-AS1 group compared with controls (Figures 2E-G and S2H). Together, these findings indicate that lncRNA *EIF1AX-AS1* suppresses EC cell proliferation *in vitro* and *in vivo*.

3.3 | *EIF1AX-AS1* induces *EIF1AX* mRNA instability

It was reported that *EIF1AX* could participate in tumorigenesis.[10] Given the sequence complementarity of *EIF1AX* with *EIF1AX-AS1*, we next explored the relationship between their expression levels. Results showed that *EIF1AX* expression was diminished after *EIF1AX-AS1* overexpression in HEC-1A and RL95-2 cells (Figure 3A,B), whereas *EIF1AX* expression was notably increased when *EIF1AX-AS1* was knocked down (Figure 3C,D).

Based on the negative correlation between the expression of lncRNA *EIF1AX-AS1* and *EIF1AX* and previous reports on the relationship between lncRNAs and their complementary mRNAs,[11] we speculated that *EIF1AX-AS1* might affect *EIF1AX* expression by regulating *EIF1AX* mRNA stability in EC. We observed decreased mRNA levels of *EIF1AX* after *EIF1AX-AS1* overexpression in the presence of actinomycin D, a transcriptional inhibitor, indicating that *EIF1AX* mRNA stability decreased after *EIF1AX-AS1* was over expressed (Figure 3E). This effect was most significant after 8 hours. Furthermore, loss of *EIF1AX-AS1* increased *EIF1AX* mRNA stability (Figure 3F). Results from RNA FISH analysis indicated that *EIF1AX-AS1* colocalized with *EIF1AX* mRNA in the cytoplasm (Figure 3G). These results indicate that *EIF1AX-AS1* regulates *EIF1AX* mRNA destabilization in EC cells.

3.4 | *EIF1AX-AS1* mediates *EIF1AX* mRNA instability by binding to PCBP1

We next examined the mechanism by which *EIF1AX-AS1* affects *EIF1AX* mRNA stability. Our data showing that *EIF1AX-AS1* was mainly located in the cytoplasm of HEC-1A and RL95-2 cells (Figure 1G) suggested that *EIF1AX-AS1* could act as a scaffold to posttranscriptionally regulate *EIF1AX* mRNA by directly interacting with specific RBPs, as observed with other lncRNAs. Thus, we used catRAPID (http://service.tartaglialab.com) to estimate potential protein-RNA pairs. We found that HNRNPQ, HNRNPD, and PCBP1 were potential RBPs that might interact with *EIF1AX-AS1*

FIGURE 4 Poly C binding protein 1 (PCBP1) binding to *EIF1AX-AS1* and *EIF1AX* mRNA. A, Silver staining SDS-PAGE gel of electrophoretically separated proteins immunoprecipitated with *EIF1AX-AS1* and its antisense RNA in HEC-1A cells. B, RNA pull-down assay was undertaken in HEC-1A and RL95-2 cells using biotinylated *EIF1AX-AS1* or antisense RNA probe transcribed *in vitro* and detected by western blotting. C, RNA immunoprecipitation (RIP) assays were undertaken in HEC-1A and RL95-2 cells using PCBP1 Ab to detect *EIF1AX-AS1* and *EIF1AX* mRNA enrichment in immunoprecipitated complexes. IgG is the negative control. *t* test: $^{**}P < .01$. D, RIP assay of the enrichment of *EIF1AX* mRNA with PCBP1 between *EIF1AX-AS1* siRNA and negative siRNA groups in EC cells. IgG was used as a negative control. *t* test: $^{**}P < .01$. E, Left panel: schematic illustration of the RNA truncates immunoprecipitated using PCBP1 Ab by improvement RIP assay. In schematic diagrams of *EIF1AX-AS1* and *EIF1AX* full-length and truncated fragments, arrow indicates the location of primers used in improvement RIP assay. Right panel: agarose gel electrophoresis was used to examine the interaction relationship among *EIF1AX-AS1*, *EIF1AX* truncates, and PCBP1in HEC-1A cells. F, G, Quantitative RT-PCR and western blot analysis were used to determine *EIF1AX* expression after PCBP1 knockdown or overexpression. *t* test: $^{**}P < .01$. H, Rate of degradation of *EIF1AX* mRNA after *PCBP1* knockdown or overexpression using RNA stability assays in EC cells. One-way ANOVA: $^{*}P < .05$. I, Rate of degradation of *EIF1AX* mRNA between the *PCBP1* overexpression group and co-treatment with *EIF1AX-AS1* shRNA and *PCBP1* overexpression plasmid group. One-way ANOVA: $^{*}P < .05$. J, Rate of degradation of *EIF1AX* mRNA between the *PCBP1* knockdown and cotransfected with *EIF1AX-AS1* overexpression and *PCBP1* shRNA plasmid. One-way ANOVA: $^{*}P < .05$. K, Left panel, after *PCBP1* knockdown and rescuing of *EIF1AX-AS1* expression, western blot analysis was used to determine EIF1AX protein levels. Right, western blot was used to determine EIF1AX protein levels after co-transfection of *EIF1AX-AS1* shRNA and *PCBP1* overexpression plasmid. Bars indicate SD. ActD, actinomycin D

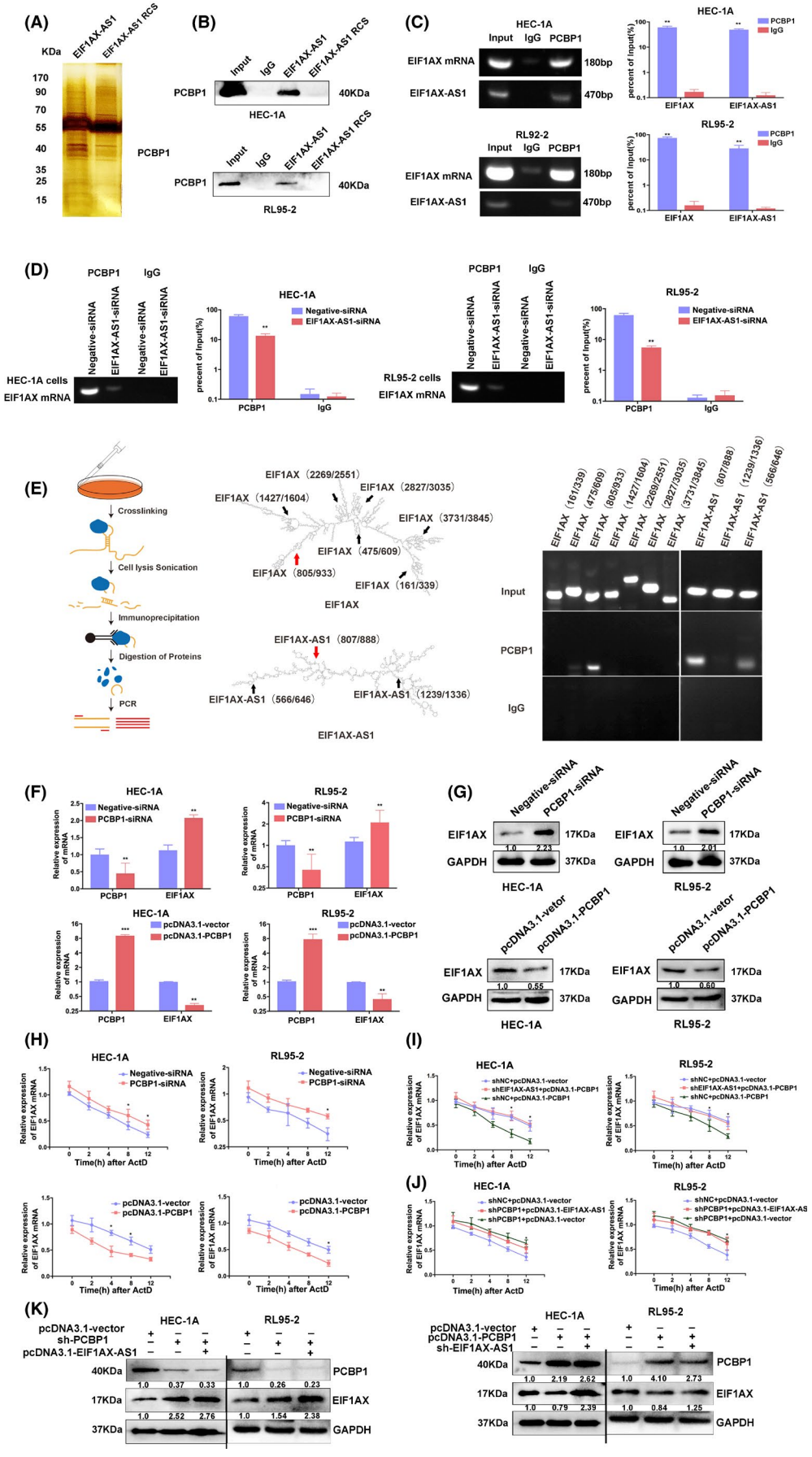
(A)
EIF1AX-AS1
EIF1AX-AS1 RCS
KDa
170
90
70
55
40
35
25
15
PCBP1
(B)
Input
IgG
EIF1AX-AS1
EIF1AX-AS1 RCS
PCBP1
40KDa
HEC-1A
RL95-2
(C)
HEC-1A
Input IgG PCBP1
EIF1AX mRNA
EIF1AX-AS1
180bp
470bp
RL92-2
percent of Input(%)
PCBP1
IgG
EIF1AX
EIF1AX-AS1
RL95-2
(D)
PCBP1
IgG
Negative-siRNA
EIF1AX-AS1-siRNA
HEC-1A cells
EIF1AX mRNA
precent of Input(%)
RL95-2 cells
(E)
Crosslinking
Cell lysis Sonication
Immunoprecipitation
Digestion of Proteins
PCR
EIF1AX (2269/2551)
EIF1AX (2827/3035)
EIF1AX (1427/1604)
EIF1AX (3731/3845)
EIF1AX (475/609)
EIF1AX (805/933)
EIF1AX (161/339)
EIF1AX
EIF1AX-AS1 (807/888)
EIF1AX-AS1 (566/646)
EIF1AX-AS1 (1239/1336)
EIF1AX-AS1
Input
PCBP1
IgG
(F)
Negative-siRNA
PCBP1-siRNA
Relative expression of mRNA
pcDNA3.1-vector
pcDNA3.1-PCBP1
(G)
Negative-siRNA
PCBP1-siRNA
EIF1AX
GAPDH
17KDa
37KDa
1.0
2.23
2.01
pcDNA3.1-vetor
pcDNA3.1-PCBP1
0.55
0.60
(H)
Relative expression of EIF1AX mRNA
Time(h) after ActD
(I)
shNC+pcDNA3.1-vector
shEIF1AX-AS1+pcDNA3.1-PCBP1
shNC+pcDNA3.1-PCBP1
(J)
shNC+pcDNA3.1-vector
shPCBP1+pcDNA3.1-EIF1AX-AS1
shPCBP1+pcDNA3.1-vector
(K)
pcDNA3.1-vector
sh-PCBP1
pcDNA3.1-EIF1AX-AS1
40KDa
17KDa
37KDa
PCBP1
EIF1AX
GAPDH
1.0 0.37 0.33
1.0 2.52 2.76
1.0 0.26 0.23
1.0 1.54 2.38
pcDNA3.1-PCBP1
sh-EIF1AX-AS1
1.0 2.19 2.62
1.0 0.79 2.39
1.0 4.10 2.73
1.0 0.84 1.25

(Figure S3A). It was found that *PCBP1* knockdown resulted in a notable increased of *EIF1AX* mRNA, as determined using RT-qPCR assays, compared with the other potential RBPs (Figure S3B).

Poly C binding protein 1 belongs to the hnRNP family that contains three hnRNP KH structural domains for binding to specific elements of target mRNAs with AU-rich elements or U-rich elements located in 3′-UTRs[12] or 5′-UTRs[13] and regulates gene expression. To further determine the relationship between *EIF1AX*, *EIF1AX-AS1*, and PCBP1, we used the RNA-protein interaction prediction website RPISeq (http://pridb.gdcb.iastate.edu/RPISeq/). The results suggested a potential interaction between *EIF1AX*, *EIF1AX-AS1*, and PCBP1 (Figure S3C).

We next undertook RNA pull-down with PCBP1 Abs to evaluate the interaction between *EIF1AX-AS1* with PCBP1. As shown in Figure 4(A,B), PCBP1 was coprecipitated with synthesized sense *EIF1AX-AS1* but not the antisense *EIF1AX-AS1* in HEC-1A and RL95-2 cells. RNA immunoprecipitation assay was then carried out using an Ab directly against PCBP1. A significant enrichment of *EIF1AX-AS1* or *EIF1AX* with PCBP1 was identified, and *EIF1AX-AS1* knockdown reduced the interaction between PCBP1 and *EIF1AX* mRNA in HEC-1A and RL95-2 cells (Figure 4C,D).

To determine the regions required for the interactions between *EIF1AX*, *EIF1AX-AS1*, and PCBP1, we used RIP assays and found that one of three regions (842-901 nt) of *EIF1AX-AS1*, predicted by catRAPID, was required for its interaction with PCBP1. We further found that the 805-933 nt region of *EIF1AX*, but not the region predicted by catRAPID, was required for association with PCBP1 in HEC-1A cells (Figures 4E and S3D,E). These results further illustrate the close regulatory relationship among *EIF1AX*, *EIF1AX-AS1*, and PCBP1.

Finally, we examined the effect of PCBP1 on *EIF1AX*. Downregulation of *PCBP1* increased *EIF1AX* expression in HEC-1A and RL95-2 cells, whereas forced expression *PCBP1* decreased *EIF1AX* expression in HEC-1A and RL95-2 cells (Figures 4F,G and S3F,G). Moreover, results of actinomycin D treatment recommend that forced expression of *PCBP1* decreased *EIF1AX* mRNA levels and facilitated its destabilization (Figure 4H), whereas loss of *PCBP1* increased *EIF1AX* mRNA levels and impeded its destabilization. Additionally, knockdown of *EIF1AX-AS1* abrogated the induction of *EIF1AX* mRNA destabilization caused by *PCBP1* overexpression (Figure 4I), and *EIF1AX-AS1* overexpression could not eliminate the effect of *PCBP1* knockdown on *EIF1AX* mRNA (Figure 4J), consistent with western blot results (Figure 4K). Based on these results, we conclude that *EIF1AX-AS1* causes the destabilization of *EIF1AX* mRNA by binding to PCBP1.

3.5 | *EIF1AX-AS1* promotes EC cell apoptosis by downregulating *EIF1AX* expression

To determine whether *EIF1AX-AS1* promotes EC cell apoptosis by regulating *EIF1AX* expression, we explored the roles of *EIF1AX-AS1* and *EIF1AX* in the proliferation and apoptosis of EC cells. *EIF1AX* expression abrogated the proliferative capacity of EC cells impaired by *EIF1AX-AS1* overexpression, as determined by CCK-8 proliferation assays (Figures 5A and S4A). Annexin V staining assay further showed that *EIF1AX* overexpression abrogated the apoptotic cell death induced by *EIF1AX-AS1* forced expression compared with controls (Figure 5B,C). Both JC-1 and western blot assays further confirmed that *EIF1AX* overexpression reduced EC cell apoptosis caused by *EIF1AX-AS1* overexpression compared with controls (Figures 5D and S4B). These results indicate that *EIF1AX-AS1* facilitates EC cell apoptosis by impaired *EIF1AX* expression, rather than through the cell cycle (Figure S4C,D).

In addition, RT-qPCR and western blot results also showed that overexpression of *EIF1AX-AS1* lacking a binding site for PCBP1 (842-901 nt) could not promote *EIF1AX* mRNA degradation (Figure S5A,B). Compared with the pcDNA3.1-EIF1AX-AS1 group, cell proliferation and cell apoptosis were restored in the pcDNA3.1-EIF1AX-AS1 mut group (Figure S5C-E). RNA pulldown also indicated that *EIF1AX* mRNA lacking the binding site (805-933 nt) could not combine with PCBP1 (Figure S5F).

We next examined the relation between *EIF1AX-AS1* and *EIF1AX* in EC *in vivo*. We subcutaneously injected *EIF1AX-AS1* overexpression cells or *EIF1AX-AS1* and *EIF1AX* co-overexpression cells into nude mice. After several weeks of observation, we found that tumor volumes and weights were lower in the LV-EIF1AX-AS1 group compared with the other groups (Figure 5E,F). Taken together, these findings indicate that lncRNA *EIF1AX-AS1* suppresses the impaired EC cell proliferation caused by *EIF1AX in vitro* and *in vivo*.

3.6 | EIF1AX increases c-Myc translation by binding YBX-1

To further examine how *EIF1AX* regulates apoptosis in EC, we undertook coimmunoprecipitation experiments followed by liquid chromatography-tandem mass spectrometry to identify proteins associated with EIF1AX. Significant interactors compared with the IgG control were analyzed by using GO and the KEGG pathway database. Interestingly, except for "protein function about translation initiation", "ribosomal complex", and "regulation of mRNA

FIGURE 5 *EIF1AX-AS1* promotes endometrial cancer (EC) cell apoptosis by downregulating *EIF1AX* expression. A, CCK-8 assay detected EC cell proliferation at the indicated times. OD, optical density. B-D, After *EIF1AX-AS1* overexpression alone or *EIF1AX-AS1* and *EIF1AX* simultaneous overexpression, cell apoptosis of HEC-1A and RL95-2 cells were detected by annexin V-FITC and JC-1, respectively. Scale bar = 100 μm. E, Nude mice were given xenografts of 5×10^6 HEC-1A cells. Tumors were dissected and photographed after approximately 4 weeks (n = 5 per group). F, Tumor weights and volumes in each group. One-way ANOVA: ns, $P > .05$; *$P < .05$; **$P < .01$; ***$P < .001$. Bars indicate SD

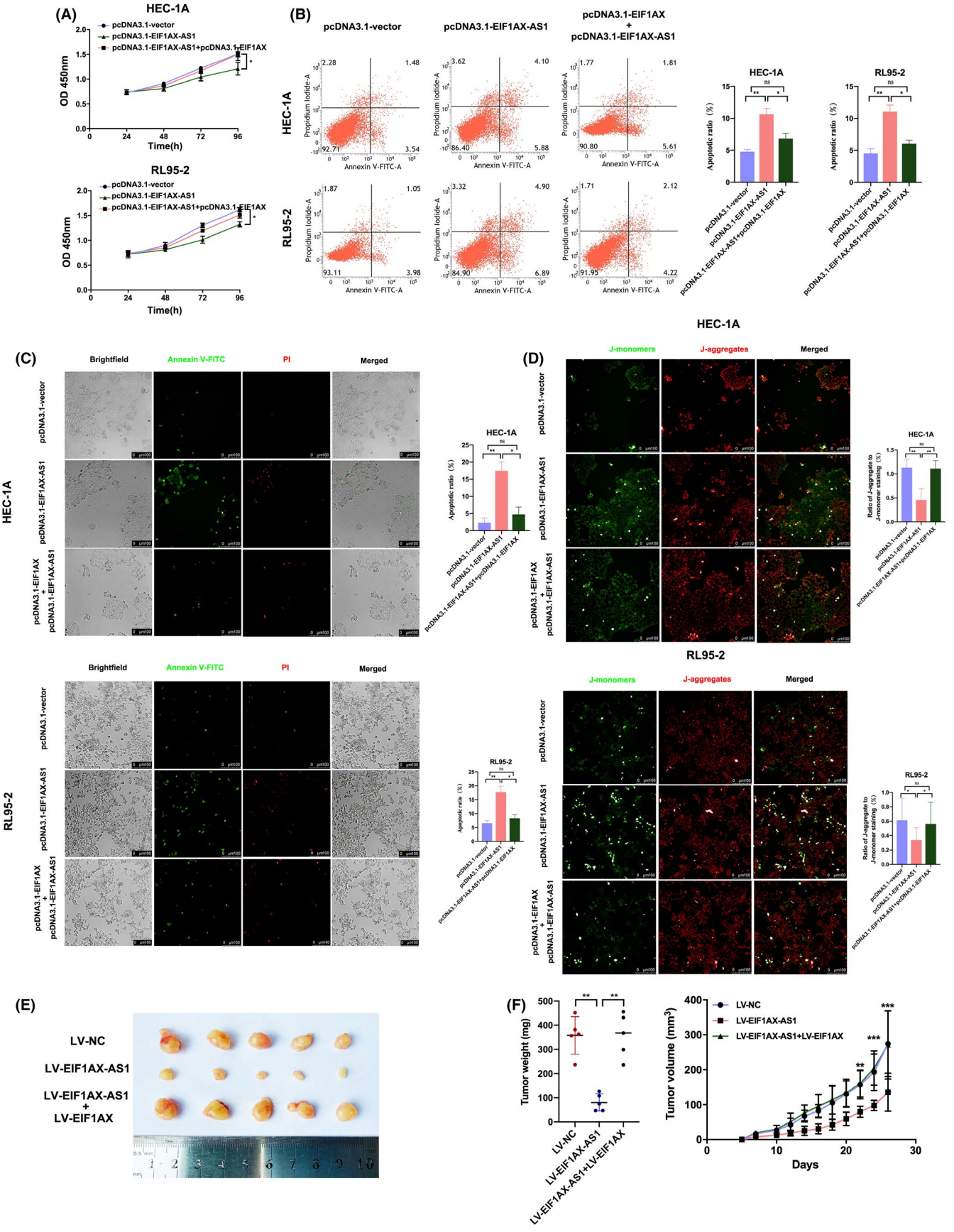

stability", GO terms associated with "internal ribosomal entry sites (IRESs)", caught our attention among these protein biological processes (Figure S6A,B). It has reported that IRES could serve as an alternative mechanism for protein production. Our results identified YBX-1 as a potential binding protein to EIF1AX (50-117 aa) (Figure S6C,D). Previous studies showed that YBX-1 functions as an

IRES trans-acting factor that upregulates c-Myc expression,[14] and *c-Myc* is closely associated with apoptosis.[15] We thus hypothesized that EIF1AX binds to YBX-1 as an IRES trans-acting factor resulting in IRES-mediated translation of c-Myc, which results in apoptosis in EC cells.

We next investigated whether EIF1AX influenced the translation of c-Myc by binding to YBX-1. We confirm that downregulating either *EIF1AX* or *YBX-1* in EC cells resulted in a decrease in c-Myc protein expression levels but not *c-Myc* mRNA levels (Figure S6E,F). Moreover, the results indicate that knockdown of *YBX-1* partially rescued the effect of forced expression of *EIF1AX* on the expression of c-Myc, BCL-2, and BAX (Figure S6G). Taken together, these results indicate that EIF1AX could regulate c-Myc expression at the translational level rather than the transcriptional level, and EIF1AX increases the translation of c-Myc by binding to YBX-1, affecting apoptosis in EC cells.

To further confirm the hypothesis that EIF1AX regulates c-Myc expression at the translational level, we undertook experiments in *EIF1AX* forced expression or knockdown cells that were pretreated with the protein synthesis inhibitor CHX. As shown in Figure S6(H,I), decreased protein levels of c-Myc were observed in *EIF1AX* silenced cells that were pretreated with CHX and increased protein levels of c-Myc were observed in cells with *EIF1AX* forced expression after treatment with CHX. This effect was most significant after 30 minutes, indicating that the translation of c-Myc was likely affected by EIF1AX. To exclude the possibility that EIF1AX affects c-Myc expression through proteasome-dependent degradation, we carried out experiments using the proteasome inhibitor MG132. We confirmed that MG132 treatment resulted in no detectable change in c-Myc protein levels in the *EIF1AX* forced expression or knockdown cells (Figure S6J,K). Together, these results show that EIF1AX increases c-Myc protein levels independent of degradation or post-translational control.

We next examined whether *c-Myc* was closely associated with apoptosis in EC cells. Loss of *c-Myc* increased *BAX* expression and decreased *BCL-2* expression in HEC-1A and RL95-2 cells, whereas forced expression *c-Myc* decreased *BAX* expression and increased *BCL-2* expression in HEC-1A and RL95-2 cells (Figure S7A-C). Taken together, these results implied that EIF1AX increases the translation of c-Myc by binding to YBX-1, affecting apoptosis in EC cells. Interestingly, the results of ChIP-seq, ChIP-qPCR, and luciferase reporter assay found that the region from −235 to 177 bp contains essential components required for maximal promoter activity, and c-Myc significantly promote *EIF1AX* promoter activity in this region in EC cells (Figure S7D-G). c-Myc could bind to the *EIF1AX* promoter and promote the transcription of *EIF1AX*, establishing a positive feed-forward (feedback) loop.

4 | DISCUSSION

Endometrial cancer has continued to show increasing incidence and diagnosis rates.[16] Recent studies have shown the utility of lncRNAs as potential tumor markers and new targets for therapy of various cancers.[17] Long noncoding RNAs regulate gene expression and protein function through a variety of molecular mechanisms, with roles in transcriptional interference, RNA splicing, and miRNA deactivation, as well as through direct interactions with transcription factors and RBPs.[18] Previous studies have revealed key roles for lncRNAs in EC. For example, lncRNA *DLEU1* binds to mTOR and increases the expression of the PI3K/AKT/mTOR pathway to promote tumorigenesis and progression of EC.[19] Therefore, screening differentially expressed lncRNAs in EC and paracancerous tissues by RNA-seq could provide new ideas for the treatment of this tumor. In the current study, we found that the lncRNA *EIF1AX-AS1* was expressed at lower levels in EC than in adjacent benign tissue and was correlated with poor survival of EC patients. Overexpression of *EIF1AX-AS1* led to a decrease in *EIF1AX* expression level, accompanied by suppressed proliferation in EC cells. These findings could provide new insights into EC.

EIF1AX promotes the formation of the ternary complex of eIF2/GTP/Met-tRNA, which binds to the 40S ribosomal subunit to form the 43S preinitiation complex and works with EIF1 to promote ribosome scanning and initiation codon selection to initiate protein translation.[20,21] Kaplan-Meier survival analysis of 5143 breast cancer cases revealed that elevated EIF1AX expression was positively associated with poor survival in breast cancer patients.[10] In addition, *EIF1AX* mutations can lead to the development of uveal melanoma.[22] These results suggest that EIF1AX is not only involved in protein translation in tumor cells, but might also be closely related to tumor proliferation and migration. Krishnamoorthy et al reported that *EIF1AX* mutations were accompanied by changes in c-Myc expression in uveal melanoma.[23] In the present study, decrease of *c-Myc* protein expression induced EC cell apoptosis after *EIF1AX* knockdown (Figure S6E,F). Yu et al reported that *c-Myc* expression was reduced in endometrioid adenocarcinoma and was accompanied by increased expression of caspase-3.[24] Our data also showed that knockdown of *c-Myc* expression led to a significant increase in *BAX* expression, accompanied by a decrease in *BCL-2* expression (Figure S7A-C). It suggests that *EIF1AX* could affect apoptosis through *c-Myc* in EC cells (Figure 6).

Interestingly, we found that EIF1AX interacts with YBX-1 to promote c-Myc translation through the IRES pathway (Figure S6). Most eukaryotic mRNAs are translated in a cap-dependent fashion. However, under oxygen deprivation and nutrient limitation conditions, the cap-independent translation driven by IRES can serve as an alternative mechanism for protein production.[25,26] In addition, this mechanism could be exploited by tumor cells to continuously promote their proliferation. EIF1AX also interacts with other IRES-related proteins in addition to YBX-1. We anticipate that future studies will identify other IRES-related proteins that are closely associated with EIF1AX-regulated apoptosis.

Our RIP assay results showed that PCBP1 binds *EIF1AX* mRNA. Poly C binding protein 1 is an RBP and member of the hnRNP family, which contains three KH structural domains that are essential for binding RNA.[27,28] Poly C binding protein 1 plays an important role in

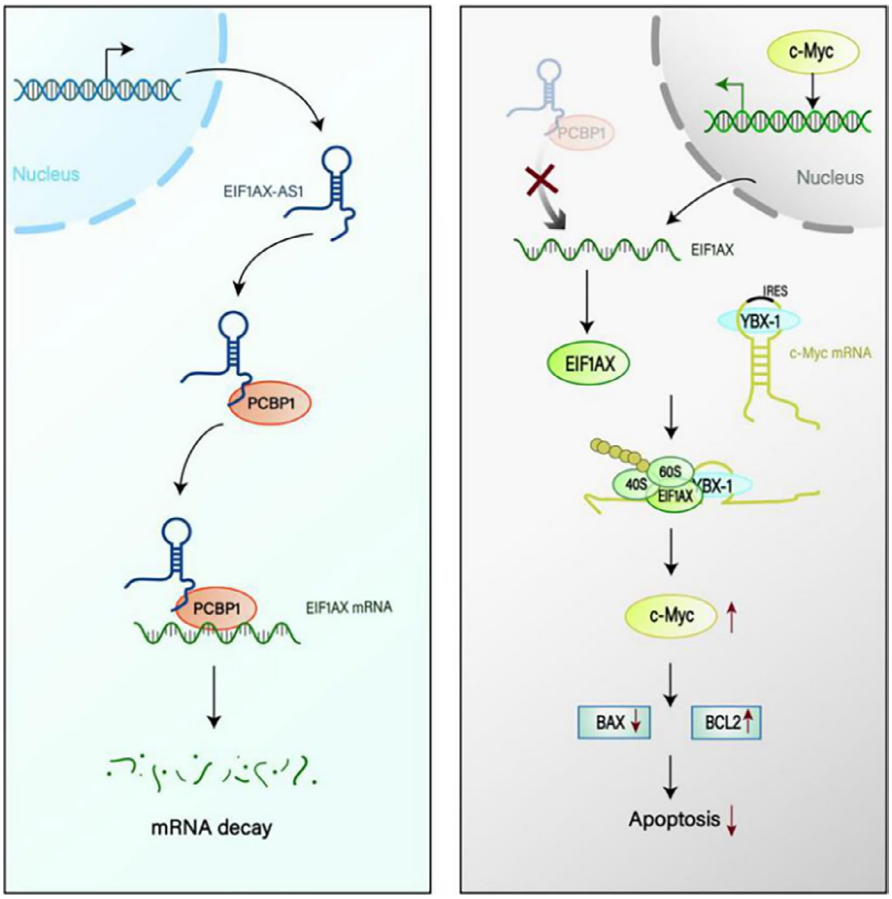

FIGURE 6 Diagram of the mechanism by which long noncoding RNA (lncRNA) *EIF1AX-AS1* affects apoptosis in endometrial cancer (EC) cells. Expression of lncRNA *EIF1AX-AS1* in EC cells reduces the degradation of *EIF1AX* mRNA by poly C binding protein 1 (PCBP1), and EIF1AX interacts with Y-box binding protein 1 (YBX-1) to promote the translation of c-Myc, which enhances cell proliferation. In addition, c-Myc binds to the *EIF1AX* promoter and promotes the transcription of *EIF1AX*, establishing a positive feed-forward (feedback) loop

mRNA stabilization,[29,30] translation activation,[31,32] and translation silencing.[33,34] Studies have shown that PCBP1 binds AU-rich elements or U-rich elements in the 3′-UTR of target mRNAs to regulate their expression.[35] In addition, PCBP1 deletion can lead to tumorigenesis. *THAP11* regulates *CD44 v6* expression through interacting with PCBP1 to inhibit *CD44 v6* expression and cell invasion in liver cancer cell lines.[36] Transforming growth factor-β1 promotes epithelial-to-mesenchymal transition and stemness of prostate cancer cells by inducing PCBP1 degradation.[37] Our results showed that PCBP1 interacts with both *EIF1AX* mRNA and *EIF1AX-AS1* to promote EC cell apoptosis by promoting *EIF1AX* mRNA degradation (Figures 4C,D and 6). Notably, Shi et al reported that PCBP1 depletion promotes tumorigenesis through attenuation of *p27* mRNA stability.[38] Zhang et al reported that PCBP1 regulates *p62/SQSTM1* mRNA stability,[39] and we confirm that PCBP1 regulates the stability of *EIF1AX* mRNA (Figure 6). Insulin-like growth factor 2 mRNA binding protein 1 is another RBP. Hämmerle et al reported that IGF2BP1 acts as an adaptor protein that recruits the CCR4-NOT complex and thereby initiates the degradation of *HULC*.[40] Zhang et al reported that IGF2BP1 recognizes m6A sites in the 3′-UTR of paternally expressed gene 10 (PEG10) mRNA to enhance its stability,[41] suggesting that RBPs perform different functions in different cell lines. Future investigations are required to elucidate how PCBP1 affects the degradation of *EIF1AX* mRNA.

Long noncoding RNAs could originate from different regions of the genome, including the sense or antisense strands of protein-coding genes, intron or exon regions of protein-coding genes, or even as independent transcripts within and outside of protein-coding genes.[42,43] *EIF1AX-AS1* is an antisense lncRNA derived from the intron region of *EIF1AX*. In NCBI and the LNCipedia database, the full length *EIF1AX-AS1* is 378 nt and includes two exons (exon 1, 268 nt; exon 2, 110 nt) and one intron (99 nt) between the exons. In this study, the full length of *EIF1AX-AS1* was 1466 nt and no intron (Figure 1E). One possible reason for these differences is the use of different cell lines, which might result in different splice variants of lncRNA. For example, Li et al reported that the length of *ZEB1-AS1* is 2449 nt[44] and Su et al reported that its length is 2535 nt;[45] both lengths were different from the NCBI database (2568 nt). Although several lncRNAs have been functionally annotated in the LNCipedia database, most lncRNAs remain uncharacterized.[46] This study provides a new perspective about lncRNAs and bioinformatics databases.

ACKNOWLEDGMENTS

The work was supported by the Science and Technology Innovation Foundation of Fujian Province (2017Y9114) and Startup Fund for Scientific Research of Fujian Medical University (2018QH2016). We thank the staff of the public technical service center of Fujian Medical University for technical assistance.

DISCLOSURE

None of the authors have any conflict of interest to declare.

ORCID

Shie Wang https://orcid.org/0000-0001-6399-7037

REFERENCES

1. Bray F, Ferlay J, Soerjomataram I, Siegel RL, Torre LA, Jemal A. Global cancer statistics 2018: GLOBOCAN estimates of incidence and mortality worldwide for 36 cancers in 185 countries. *CA Cancer J Clin*. 2018;68:394-424.
2. Siegel RL, Miller KD, Jemal A. Cancer statistics, 2020. *CA Cancer J Clin*. 2020;70:7-30.
3. Batista PJ, Chang HY. Long noncoding RNAs: cellular address codes in development and disease. *Cell*. 2013;152:1298-1307.
4. Xu Q, Lin YB, Li L, Liu J. LncRNA TLR8-AS1 promotes metastasis and chemoresistance of ovarian cancer through enhancing TLR8 mRNA stability. *Biochem Biophys Res Commun*. 2020;526:857-864.
5. Lan Y, Xiao X, He Z, et al. Long noncoding RNA OCC-1 suppresses cell growth through destabilizing HuR protein in colorectal cancer. *Nucleic Acids Res*. 2018;46:5809-5821.
6. Lee S, Kopp F, Chang TC, et al. Noncoding RNA NORAD regulates genomic stability by sequestering PUMILIO proteins. *Cell*. 2016;164:69-80.
7. Wang A, Bao Y, Wu Z, et al. Long noncoding RNA EGFR-AS1 promotes cell growth and metastasis via affecting HuR mediated mRNA stability of EGFR in renal cancer. *Cell Death Dis*. 2019;10:154.
8. Huang J, Ke P, Guo L, et al. Lentivirus-mediated RNA interference targeting the long noncoding RNA HOTAIR inhibits proliferation and invasion of endometrial carcinoma cells *in vitro* and *in vivo*. *Int J Gynecol Cancer*. 2014;24:635-642.
9. Sun J, Wang D, Lin J, et al. Icariin protects mouse Leydig cell testosterone synthesis from the adverse effects of di(2-ethylhexyl) phthalate. *Toxicol Appl Pharmacol*. 2019;378:114612.
10. Li Y, Guo L, Ying S, Feng GH, Zhang Y. Transcriptional repression of p21 by EIF1AX promotes the proliferation of breast cancer cells. *Cell Prolif*. 2020;53:e12903.
11. Mo S, Zhang L, Dai W, et al. Antisense lncRNA LDLRAD4-AS1 promotes metastasis by decreasing the expression of LDLRAD4 and predicts a poor prognosis in colorectal cancer. *Cell Death Dis*. 2020;11:155.
12. Giles KM, Daly JM, Beveridge DJ, et al. The 3'-untranslated region of p21WAF1 mRNA is a composite cis-acting sequence bound by RNA-binding proteins from breast cancer cells, including HuR and poly(C)-binding protein. *J Biol Chem*. 2003;278:2937-2946.
13. Wang H, Vardy LA, Tan CP, et al. PCBP1 suppresses the translation of metastasis-associated PRL-3 phosphatase. *Cancer Cell*. 2010;18:52-62.
14. Cobbold LC, Wilson LA, Sawicka K, et al. Upregulated c-myc expression in multiple myeloma by internal ribosome entry results from increased interactions with and expression of PTB-1 and YB-1. *Oncogene*. 2010;29:2884-2891.
15. Wang X, Zhang X, Han Y, et al. Silence of lncRNA ANRIL represses cell growth and promotes apoptosis in retinoblastoma cells through regulating miR-99a and c-Myc. *Artif Cells Nanomed Biotechnol*. 2019;47:2265-2273.
16. Amant F, Moerman P, Neven P, Timmerman D, Van Limbergen E, Vergote I. Endometrial cancer. *Lancet*. 2005;366:491-505.
17. Cancer Genome Atlas Research Network, Albert Einstein College of Medicine, Analytical Biological Services, et al. Integrated genomic and molecular characterization of cervical cancer. *Nature*. 2017;543:378-384.
18. Wapinski O, Chang HY. Long noncoding RNAs and human disease. *Trends Cell Biol*. 2011;21:354-361.
19. Du Y, Wang L, Chen S, Liu Y, Zhao Y. lncRNA DLEU1 contributes to tumorigenesis and development of endometrial carcinoma by targeting mTOR. *Mol Carcinog*. 2018;57:1191-1200.
20. Hinnebusch AG. Molecular mechanism of scanning and start codon selection in eukaryotes. *Microbiol Mol Biol Rev*. 2011;75(3):434-467, first page of table of contents.
21. Pestova TV, Borukhov SI, Hellen CU. Eukaryotic ribosomes require initiation factors 1 and 1A to locate initiation codons. *Nature*. 1998;394:854-859.
22. Ewens KG, Kanetsky PA, Richards-Yutz J, et al. Chromosome 3 status combined with BAP1 and EIF1AX mutation profiles are associated with metastasis in uveal melanoma. *Invest Ophthalmol vis Sci*. 2014;55:5160-5167.
23. Krishnamoorthy GP, Davidson NR, Leach SD, et al. EIF1AX and RAS mutations cooperate to drive thyroid tumorigenesis through ATF4 and c-MYC. *Cancer Discov*. 2019;9:264-281.
24. Yu N, Zhang T, Zhao D, Cao Z, Du J, Zhang Q. CIP2A is overexpressed in human endometrioid adenocarcinoma and regulates cell proliferation, invasion and apoptosis. *Pathol Res Pract*. 2018;214:233-239.
25. Andreev DE, O'Connor PB, Fahey C, et al. Translation of 5' leaders is pervasive in genes resistant to eIF2 repression. *Elife*. 2015;4:e03971.
26. Spriggs KA, Bushell M, Willis AE. Translational regulation of gene expression during conditions of cell stress. *Mol Cell*. 2010;40:228-237.
27. Ferre F, Colantoni A, Helmer-Citterich M. Revealing protein-lncRNA interaction. *Brief Bioinform*. 2016;17:106-116.
28. Kiledjian M, Wang X, Liebhaber SA. Identification of two KH domain proteins in the alpha-globin mRNP stability complex. *EMBO J*. 1995;14:4357-4364.
29. Holcik M, Liebhaber SA. Four highly stable eukaryotic mRNAs assemble 3' untranslated region RNA-protein complexes sharing cis and trans components. *Proc Natl Acad Sci U S A*. 1997;94:2410-2414.
30. Weiss IM, Liebhaber SA. Erythroid cell-specific determinants of alpha-globin mRNA stability. *Mol Cell Biol*. 1994;14:8123-8132.
31. Blyn LB, Towner JS, Semler BL, Ehrenfeld E. Requirement of poly(rC) binding protein 2 for translation of poliovirus RNA. *J Virol*. 1997;71:6243-6246.
32. Gamarnik AV, Andino R. Two functional complexes formed by KH domain containing proteins with the 5' noncoding region of poliovirus RNA. *RNA*. 1997;3:882-892.
33. Collier B, Goobar-Larsson L, Sokolowski M, Schwartz S. Translational inhibition *in vitro* of human papillomavirus type 16 L2 mRNA mediated through interaction with heterogenous ribonucleoprotein K and poly(rC)-binding proteins 1 and 2. *J Biol Chem*. 1998;273:22648-22656.
34. Ostareck DH, Ostareck-Lederer A, Wilm M, Thiele BJ, Mann M, Hentze MW. mRNA silencing in erythroid differentiation: hnRNP K and hnRNP E1 regulate 15-lipoxygenase translation from the 3' end. *Cell*. 1997;89:597-606.
35. Cho SJ, Jung YS, Chen X. Poly (C)-binding protein 1 regulates p63 expression through mRNA stability. *PLoS One*. 2013;8:e71724.
36. Lian WX, Yin RH, Kong XZ, et al. THAP11, a novel binding protein of PCBP1, negatively regulates CD44 alternative splicing and cell invasion in a human hepatoma cell line. *FEBS Lett*. 2012;586:1431-1438.
37. Chen Q, Gu M, Cai ZK, et al. TGF-beta1 promotes epithelial-to-mesenchymal transition and stemness of prostate cancer cells by inducing PCBP1 degradation and alternative splicing of CD44. *Cell Mol Life Sci*. 2021;78:949-962.
38. Shi H, Li H, Yuan R, et al. PCBP1 depletion promotes tumorigenesis through attenuation of p27(Kip1) mRNA stability and translation. *J Exp Clin Cancer Res*. 2018;37:187.
39. Zhang W, Zhang S, Guan W, et al. Poly C binding protein 1 regulates p62/SQSTM1 mRNA stability and autophagic degradation to repress tumor progression. *Front Genet*. 2020;11:930.
40. Hämmerle M, Gutschner T, Uckelmann H, et al. Posttranscriptional destabilization of the liver-specific long noncoding RNA HULC by the IGF2 mRNA-binding protein 1 (IGF2BP1). *Hepatology*. 2013;58:1703-1712.

41. Zhang L, Wan Y, Zhang Z, et al. IGF2BP1 overexpression stabilizes PEG10 mRNA in an m6A-dependent manner and promotes endometrial cancer progression. *Theranostics*. 2021;11:1100-1114.
42. Orom UA, Shiekhattar R. Long non-coding RNAs and enhancers. *Curr Opin Genet Dev*. 2011;21:194-198.
43. Xu JZ, Zhang JL, Zhang WG. Antisense RNA: the new favorite in genetic research. *J Zhejiang Univ Sci B*. 2018;19:739-749.
44. Li T, Xie J, Shen C, et al. Upregulation of long noncoding RNA ZEB1-AS1 promotes tumor metastasis and predicts poor prognosis in hepatocellular carcinoma. *Oncogene*. 2016;35:1575-1584.
45. Su W, Xu M, Chen X, et al. Long noncoding RNA ZEB1-AS1 epigenetically regulates the expressions of ZEB1 and downstream molecules in prostate cancer. *Mol Cancer*. 2017;16:142.
46. Volders PJ, Helsens K, Wang X, et al. LNCipedia: a database for annotated human lncRNA transcript sequences and structures. *Nucleic Acids Res*. 2013;41:D246-251.

SUPPORTING INFORMATION

Additional supporting information may be found in the online version of the article at the publisher's website.

How to cite this article: Lv C, Sun J, Ye Y, et al. Long noncoding RNA *EIF1AX-AS1* promotes endometrial cancer cell apoptosis by affecting *EIF1AX mRNA* stabilization. *Cancer Sci*. 2022;113:1277–1291. doi:10.1111/cas.15275